Chemical Engineering Journal 165 (2010) 907–915

Contents lists available at ScienceDirect

Chemical Engineering Journal

journal homepage: www.elsevier.com/locate/cej

Studies of equilibrium, kinetics simulation and thermodynamics of cAMP adsorption onto an anion-exchange resin

Wenbin Qian[b,c], Xiaoqing Lin[a,b], Xiqun Zhou[b,c], Xiaochun Chen[b,c], Jian Xiong[a,b], Jianxin Bai[a,c], Hanjie Ying[d,*]

[a] State Key Laboratory of Materials-Oriented Chemical Engineering, Nanjing 210009, PR China
[b] College of Biotechnology and Pharmaceutical Engineering, Nanjing University of Technology, Nanjing 210009, PR China
[c] National Engineering Technique Research Center for Biotechnology, Nanjing 211816, PR China
[d] College of Life Science and Pharmaceutical Engineering, Nanjing University of Technology, Xin mofan Road 5, Nanjing 210009, PR China

ARTICLE INFO

Article history:
Received 15 July 2010
Received in revised form
29 September 2010
Accepted 29 September 2010

Keywords:
Adsorption
cAMP
Effective diffusion coefficient
Fick model
Langmuir

ABSTRACT

In a batch equilibrium system, the maximum adsorption capacity of cAMP onto an anion-exchange resin reached 0.1718, 0.1956, 0.2764 and 0.3437 g g^{-1} at 283, 293, 303 and 313 K, respectively. The adsorption data obtained were well described by the Langmuir isotherm. In the batch kinetic system, Fick diffusion, pseudo first-order and pseudo second-order models were applied to simulate the experimental kinetic data. The results revealed that the Fick model best described the adsorption process, and clearly predicted the intraparticle distribution of the concentration. The effective diffusion coefficients (D_e) for 283, 293, 303 and 313 K were 0.37×10^{-10}, 0.51×10^{-10}, 0.86×10^{-10} and 1.41×10^{-10} $m^2\ s^{-1}$, respectively. The thermodynamic parameters such as ΔG^0, which were all negative, indicated that the adsorption of cAMP onto the anion-exchange resin was spontaneous and the positive value of ΔH^0 (+8.66 kJ mol^{-1}) showed that the adsorption was an endothermic reaction.

1. Introduction

Cyclic adenosine-3′,5′-monophosphate (cAMP) is an important compound in organisms, and is well-known as the "second messenger" in living cells due to its participation in various chemical reactions and its active role as a mediator to various hormones [1]. Many studies have reported that cAMP has multiple pharmacological functions such as relaxing smooth muscle, expanding blood vessels, and promoting nerve regeneration [2]. The present production of cAMP is primarily dependent on chemical synthesis, which not only involves considerable costs and complex procedures, but also has flaws such as low yield, and environmental pollution due to the use of pyridine as a solvent. With the development of microbial synthesis, microbial production of cAMP has attracted much attention because it is simple and economical compared with the complicated multistep chemical synthesis [3]. Only a small range of bacterial species are known to have the ability to produce cAMP, including *Microbacterium* sp. no. 205 (ATCC21376), *Corynebacterium murisepticum* no. 7 (ATCC21374) and *Arthrobacter* sp. no. 11 (ATCC21375) which were identified in the early 1980s by Ishiyama [4]. In 2009, Chen et al. reported that one strain of *Microbacterium* sp. no. 205 successfully produced 9.87 g L^{-1} cAMP in a 5 L fermenter [5].

However, the downstream separation processes of cAMP have never been reported. The isolation of cAMP from fermentative broth is performed in a series of steps. At the end of fermentation, the broth is first clarified by filtration or centrifugation. The most important step, primary extraction from clarified broth, is based on several two-phase separation methods. One of these methods is the direct extraction of the filtrate with organic solvent, producing an organic phase containing cAMP, which is subsequently isolated. An alternative process which avoids the use of solvent consists of chromatographic adsorption techniques with non-ionic or ionic adsorbents. This technique has developed rapidly in recent decades, mainly since the introduction of synthetic adsorbents [6]. In particular, ion-exchange adsorption, which involves electrostatic attraction of ionic components to sites on the adsorbent surface with opposite charges, can be used in many domains of the separation and purification processes and has replaced activated carbon which has long been used as a highly efficient adsorbent for the removal of numerous heavy metals from water [7]. Activated carbon suffers from a number of disadvantages. It is quite expensive and the higher the quality, the greater the cost. Both chemical and thermal regeneration of spent carbon is expensive, impractical on

* Corresponding author. Present address. Tel.: +86 25 86990001; fax: +86 25 58133398.
E-mail addresses: qianwenbin007@126.com (W. Qian), yinghanjie@njut.edu.cn (H. Ying).

1385-8947/$ – see front matter © 2010 Elsevier B.V. All rights reserved.
doi:10.1016/j.cej.2010.09.073

Nomenclature

C	concentration of cAMP at t time ($g\,L^{-1}$)
C_0	initial concentration of cAMP in aqueous solution ($g\,L^{-1}$)
C_e	concentration of cAMP at equilibrium ($g\,L^{-1}$)
C_{exp}	concentration of cAMP recorded in the experiments ($g\,L^{-1}$)
C_{pred}	concentration of cAMP predicted with the simulation ($g\,L^{-1}$)
D_e	the effective diffusion coefficient ($m^2\,s^{-1}$)
D	the average absolute deviation
m	mass of adsorbent (g)
n	Freundlich isotherm constant
N	number of experimental data points
q	mass of cAMP adsorbed per unit mass of adsorbent ($g\,g^{-1}$)
q_e	mass of cAMP adsorbed per unit mass of adsorbent at equilibrium ($g\,g^{-1}$)
q_m	maximum mass of cAMP adsorbed per unit mass of adsorbent ($g\,g^{-1}$)
$\bar{q}$	average mass of cAMP adsorbed per unit mass of adsorbent ($g\,g^{-1}$)
k_1	the rate constant of pseudo first-order kinetic model (min^{-1})
k_2	the rate constant of pseudo second-order kinetic model (min^{-1})
K_a	dissociation constant of cAMP in aqueous solution ($mol\,L^{-1}$)
K_L	Langmuir isotherm constant ($L\,g^{-1}$)
K_F	Freundlich isotherm constant ($L^{1/n}(g^{1/n-1}\,g)^{-1}$)
r	distance in radial direction of a resin particle (μm)
R	the gas constant ($J\,(mol\,K)^{-1}$)
R_p	radius of a resin particle (μm)
t	time (min or s)
T	temperature (K)
V	volume of the cAMP solution (mL)
β	a constant related to the mean free energy of adsorption per mole of the adsorbate ($mol^2\,kJ^{-2}$)
δ	distribution coefficient
δ_0	distribution coefficient of neutral cAMP
δ_1	distribution coefficient of cAMP with negative charge
ε	the Polanyi potential, which is equal to $RT\ln(1+(1/C_e))$
ΔG^0	free energy changes during the cAMP adsorption process ($kJ\,mol^{-1}$)
ΔH^0	enthalpy change during the cAMP adsorption process ($kJ\,mol^{-1}$)
ΔS^0	entropy change during the cAMP adsorption process ($J\,(mol\,K)^{-1}$)

a large scale and produces additional effluent and results in considerable loss of the adsorbent [8]. However, the ion-exchange resin is highly effective, low-cost material, efficient, and easy to operate among the physicochemical treatment processes. Furthermore, ion-exchange resin is particularly effective for treating water of heavy metals which is very common in practice [9].

Ion-exchange adsorption equilibrium and kinetics have a critical effect on the efficiency and productivity of adsorption processes. Therefore, in this work the ion-exchange equilibrium and kinetics of cAMP on an anion-exchange resin, made in our laboratory and marked as D13 resin, were investigated using batch experiments at different temperatures. Some thermodynamic adsorption parameters such as free energy, enthalpy, and entropy were estimated by correlations [10]. Values of adsorption capacity and thermodynamic parameters were the actual indicators for practical application of the process into industrial production.

In this study, Fick diffusion, pseudo first-order and pseudo second-order models were used to compare simulation of the ion-exchange kinetics of cAMP adsorption. In general, ion flux in the solid phase is commonly described by either the Fick model or the Nernst–Planck model [11]. However, the Nernst–Planck model requires individual diffusion coefficients for each ion involved in the adsorption process including counter-ions and even co-ions [12]. Reliable correlations linking resin-phase diffusion coefficients to liquid-phase diffusion coefficients are unavailable, and values referred to in the literature can be contradictory [13]. In the diffusion model namely the Fick model, the overall adsorption rate is assumed to take place by a mechanism consisting of three consecutive steps: (i) external film mass transport, (ii) intraparticle diffusion, and (iii) adsorption rate on a site inside the pores [14]. Due to the fact that the effect of the external film mass transfer resistance is negligible [15–17] compared to the effect of the intraparticle (internal) mass transfer resistance in the pores of the particles, the effect of the external film mass transfer resistance in batch experiments with porous particles will not be further considered in this work. The rate of adsorption on an active site is instantaneous, therefore the kinetics of ion exchange were typically limited by intraparticle diffusion. Therefore, effective diffusion coefficients (D_e) of cAMP at different temperatures were obtained by simulating the experimental results using the Fick model.

2. Materials and methods

2.1. Materials

A stock solution of cAMP was prepared by dissolving an accurate quantity of cAMP·H_2O in deionized water. Other concentrations prepared from the stock solution by dilution varied between 0.01 and 8 $g\,L^{-1}$ and the pH of the working solutions was adjusted to the desired values with 2 M HCl or 2 M NaOH. Fresh dilutions were used for each experiment. All the chemicals used were of analytical grade. The adsorbent used in this research was the polymeric resin D13 having basic groups, which were made in our laboratory. The resin was first cleaned of preservative agents and polymerization residuals by successive washings with ethanol and deionized water, dried in an oven, and then stored in a dessicator. The ion exchange resin used in experiments must be in Cl^- form, which means D13 resin should been soaked in 0.1 mol/L HCl solution for 8 h, and then been rinsed by deionized water. The radius of resin is 335 μm and Table 1 gives some physiochemical properties of resin D13.

2.2. The dissociation constants of cAMP

In order to determine accurate dissociation constants of cAMP, firstly a cAMP solution of a given concentration (4 $g\,L^{-1}$) and initial pH was recorded. Secondly, using the alkalimetric titration method

Table 1
Physiochemical properties of resin D13.

Matrix structure	Polystyrene
Crosslink density (%)	>20
Moisture content (%)	40–51
Hydrated density ($g\,mL^{-1}$)	1.09–1.12
Specific area ($m^2\,g^{-1}$)	658.2
Particle diameter (mm)	0.7–0.8
Pore volume ($mL\,g^{-1}$)	0.33

the pH was slowly adjusted with a volume of 0.1 mol/L NaOH solution. From the plots, dissociation constant was obtained.

2.3. The effect of pH on absorbate

The effect of pH on the adsorption of cAMP onto D13 resin was investigated by equilibrating the adsorption mixture with adsorbent and 50 mL of 5 g L^{-1} cAMP solution at different pH values between 3 and 11. These solutions (50 mL) were added to 250 mL Erlenmeyer flasks containing 1 g wet resin and the contents were equilibrated by shaking the flasks in an incubator at 200 rpm and 298 K for 8 h. The concentration of cAMP was measured by HPLC and the amount of cAMP adsorbed by the resin was calculated by subtraction.

2.4. Equilibrium experiments

Batch experiments were performed to study the ion-exchange equilibrium between cAMP and D13 resin at optimum pH and different temperatures (283 K, 293 K, 303 K and 313 K). Solutions of cAMP (0.01–8 g L^{-1}) were prepared. These solutions (50 mL) were added to 250 mL Erlenmeyer flasks containing 1 g wet resin and the contents were equilibrated by shaking the flasks in an incubator at 200 rpm for 8 h. The concentration of cAMP was measured by HPLC and the amount of cAMP adsorbed by the resin was calculated by subtraction.

$$q_e = \frac{(C_0 - C_e)V}{m} \quad (1)$$

2.5. Batch adsorption kinetics studies

Rates of ion exchange were measured in 500 mL Erlenmeyer flasks closed with glass stoppers on a magnetic stirrer at a constant temperature of 283 K, 293 K, 303 K and 313 K maintained by a thermostatic water bath. cAMP solutions (200 mL) were added to the flask and left to reach thermal equilibrium. The resin (0.4–1 g) was then quickly poured into the flask. The procedure was monitored by the periodic sampling of 0.1 mL of solution from the flasks.

On the basis of transient-state batch sorption experiments, effective diffusion coefficients of cAMP inside the adsorbent particle at different temperatures were also obtained. Effective diffusion coefficients in the adsorbent particle were then determined from the mass balance within a spherical particle (see mathematical model of the sorption process for details).

2.6. HPLC analysis

Concentrations of the cAMP solutions were determined by HPLC (System Gold, Beckman, USA) equipped with a 125 solvent module and a 166 UV-visible detector. Compounds were separated on a 250 mm × 4.6 mm i.d. C18 reversed-phase column (SepaxHP-C18, USA). The mobile phase was a 25:75 (v/v) mixture of methanol and 90 mmol L^{-1} phosphate buffer which was adjusted to pH 6.6 by triethylamine. The flow rate was 0.8 mL min^{-1} and the detection wavelength was 254 nm.

3. Results and discussion

3.1. The dissociation constant of cAMP

In 1959, Dawson et al. reported that there were two acid dissociative groups in AMP, ($-H_2PO_3$) and ($-HPO_3^-$). Their p*K*s were 3.3 and 6.1, respectively [18]. Goldberg and Tewari reported that one of the acid dissociative groups ($-H_2PO_3$) of AMP molecule had a pK_a of approximately 3.9 [19]. cAMP is the product of

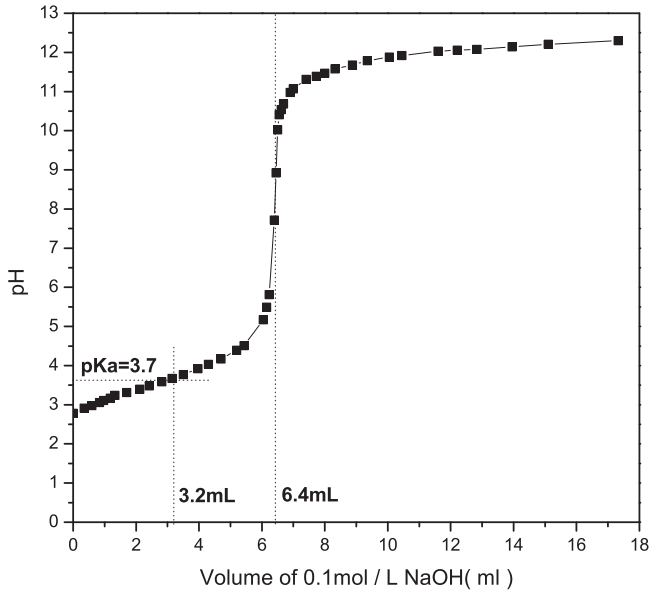

Fig. 1. The alkalimetric titration curve of 4 g L^{-1} cAMP using 0.01 mol L^{-1} NaOH.

5′-AMP intramolecular dehydration. When dehydration occurs, a hydroxyl of the phosphorus atom is reacted, leaving the group ($-HPO_3$) whose pK_a has been reported to be 3.3 [20]. In this work, it had been found that there was only one dissociation constants, and its pK_a was estimated to be 3.7 for ($-HPO_3$) by the plots of pH versus volume of 0.1 mol L^{-1} NaOH in Fig. 1. pK_a of cAMP was determined by the Henderson–Hasselbach equation (Eq. (3)) derived from the chemical reaction (Eq. (2)), which means the value of pK_a is equal to pH at the half-titration point (3.2 mL in Fig. 1) where the concentration of cAMP·H is identical to that of $cAMP^-$. As a result, it was proved that the obtained value of pK_a basically approaches the one reported in literature.

$$cAMP \cdot H + NaOH \rightleftharpoons cAMP^- + Na^+ + H_2O\,(aq.) \quad (2)$$

$$pH = pK_a + \log \frac{[cAMP^-]}{[cAMP \cdot H]} \quad (3)$$

3.2. Effect of pH on cAMP uptake

The study was also carried out as Eq. (4) for Cl^-/$cAMP^-$ system for the different temperatures in the range of 283–313 K. Only cAMP with negative charge can be exchanged with Cl^- instantly. Therefore, it is necessary to research the effect of pH on cAMP dissociation extent.

$$R{-}Cl + cAMP^- \rightarrow R{-}cAMP + Cl^-\,(aq.) \quad (4)$$

The effect of pH on the adsorption process is shown in Fig. 2. The amount of cAMP adsorbed per unit mass of the adsorbent material (g g^{-1}) at equilibrium and 293 K dramatically increased with an increase in pH between 3.0 and 5.0, increased slowly with an increase in pH between 5.0 and 8.0, and then reached a maximum value of 0.206 g g^{-1} when the pH was 8.0. From pH 9.0 to 11.0, the adsorption capacity became smaller, and was attributed to the high concentration of OH^- which competed with negative cAMP molecular in the ion exchange process. Because cAMP is a weak monoacid, it may exist in two forms of $cAMP^-$ ion and cAMP molecule. Their distribution coefficients in aqueous solution can be represented by

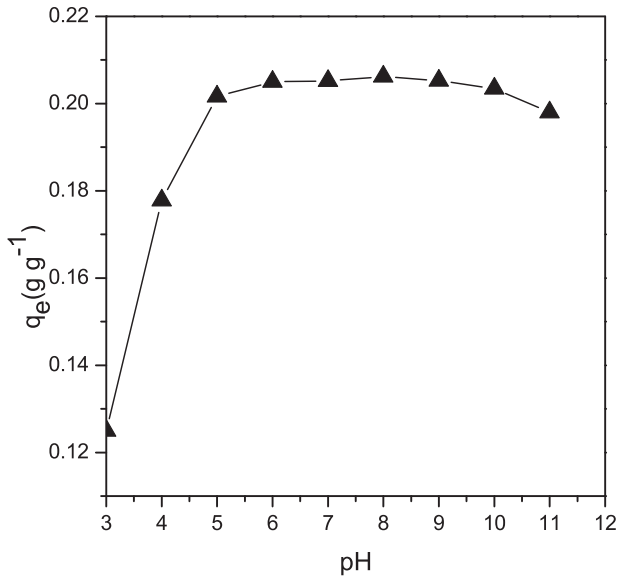

Fig. 2. The adsorption capacity of D13 resin at different pH values of cAMP solutions at 293 K.

following equations, respectively

$$\delta_0 = \frac{[\text{cAMP}\cdot\text{H}]}{[\text{cAMP}\cdot\text{H}]+[\text{cAMP}^-]} = \frac{1}{1+([\text{cAMP}^-]/[\text{cAMP}\cdot\text{H}])} = \frac{1}{1+(K_a/[\text{H}^+])} = \frac{[\text{H}^+]}{[\text{H}^+]+K_a} \quad (5)$$

$$\delta_1 = \frac{[\text{cAMP}^-]}{[\text{cAMP}\cdot\text{H}]+[\text{cAMP}^-]} = \frac{K_a}{[\text{H}^+]+K_a} \quad (6)$$

From Fig. 3 charted by plotting δ versus pH, it is obvious that cAMP with negative charge absolutely dominates in two forms when the value of pH is above 7.0 which basically corresponded the optimal value 8.0 that was adopted in other else experiments.

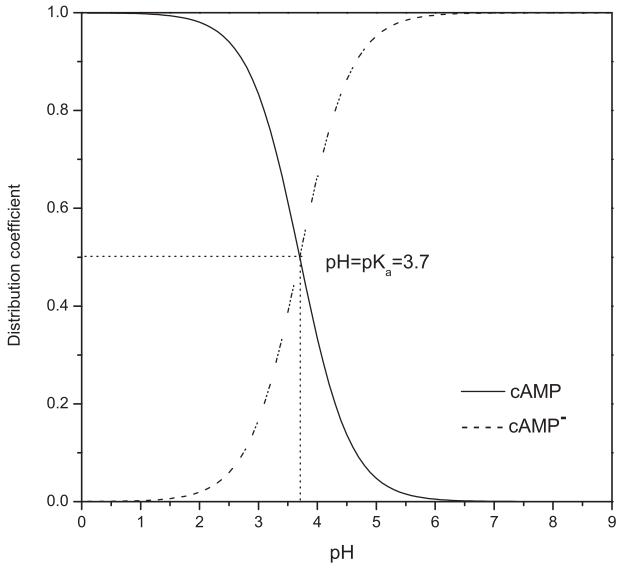

Fig. 3. The distribution coefficients of two forms of cAMP molecular in aqueous solutions of variable pH.

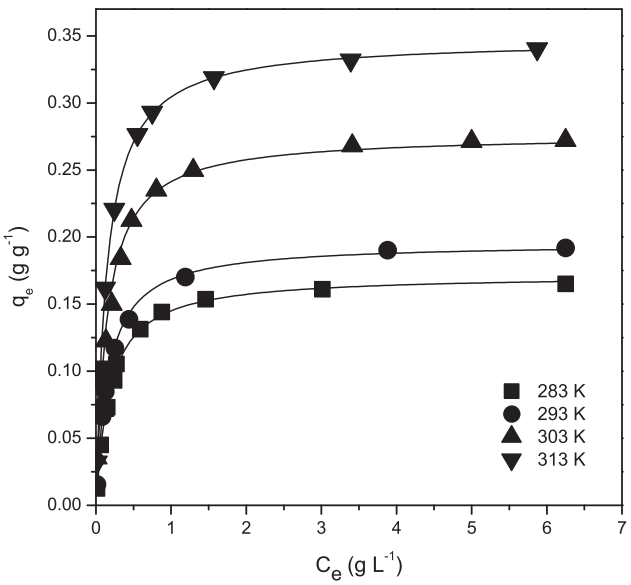

Fig. 4. Fitting of experimental data to Langmuir equation.

3.3. Adsorption isotherms

The adsorption data were analyzed to determine whether the isotherm obeyed the Langmuir, Freundlich and Dubinin–Radushkevich isotherm models which are represented by the following equations [21–23]:

Langmuir:

$$q_e = \frac{q_m K_L C_e}{1+K_L C_e} \quad (7)$$

Freundlich:

$$q_e = K_F C_e^{1/n} \quad (8)$$

Dubinin–Radushkevich (D–R):

$$q_e = q_m e^{-\beta\varepsilon^2} \quad (9)$$

The values of the Langmuir constants q_m, and K_L with the correlation coefficient are listed in Table 2 for the adsorption of cAMP onto D13 and the theoretical Langmuir isotherm is plotted in Fig. 4 together with the experimental data points. The value of the correlation coefficient is higher than the other two isotherm values. At each temperature, the Langmuir equation represents the best fit of experimental data. The Langmuir model is the best-known isotherm for describing adsorption from an aqueous solution. The Langmuir model assumes that there is no interaction between the adsorbate molecules. The adsorption is localized in a monolayer. The monolayer saturation capacity q_m was 0.1718, 0.1956, 0.2764 and 0.3437 g g^{-1} for 283, 293, 303 and 313 K, respectively and q_m increased with an increase in temperature.

The effect of isotherm shape has been discussed with a view for predicting whether an adsorption system is favorable or unfavorable [24]. The essential feature of the Langmuir isotherm can be expressed by means of 'R_L', a dimensionless constant referred to as the separation factor or equilibrium parameter K_L and can be calculated using the following equation

$$R_L = \frac{1}{1+K_L C_0} \quad (10)$$

The values of R_L calculated using the above equation are listed in Table 2. As the R_L values lie between 0 and 1, the related adsorption process was favorable [24,25]. Furthermore, the R_L values for

Table 2
Isotherm parameters and correlation coefficient r^2.

T (K)	Langmuir			Freundlich			Dubinin–Radushkevich (D–R)		
	K_L (L g^{-1})	q_m (g g^{-1})	r^2	K_F (L$^{1/n}$(g$^{1/n-1}$ g)$^{-1}$)	n	r^2	q_m (g g^{-1})	β ($\times 10^{-8}$ mol^2 kJ^{-2})	r^2
283	5.4001	0.17181	0.9975	0.1249	0.2336	0.9245	2.825	1.11	0.5894
293	6.1884	0.19563	0.9974	0.1411	0.2222	0.9436	1.939	1.22	0.6732
303	6.8876	0.27637	0.9914	0.2057	0.2126	0.9405	1.329	1.30	0.6212
313	7.7107	0.34377	0.9989	0.2599	0.2282	0.9171	1.119	1.35	0.5862

cAMP onto D13 resin were between 2.53×10^{-2} and 3.57×10^{-2}, therefore, cAMP adsorption was favorable.

3.4. Adsorption kinetics

3.4.1. The Fick model

It was assumed that ion exchange occurred between spherical ion exchangers of uniform size. The ion-exchange kinetics model was simplified by making four further assumptions: (1) the resin was treated as a quasi-homogenous phase; (2) the flux of the co-ion was neglected; (3) diffusion was restricted to radial diffusion; and (4) intraparticle diffusion was the rate-limiting step throughout the process.

The Fick equation for the flux of cAMP ions was written as

$$\frac{\partial q}{\partial t} = D_e \left(\frac{\partial^2 q}{\partial r^2} + \frac{2}{r} \frac{\partial q}{\partial r} \right) \tag{11}$$

The initial and boundary conditions are given as

$$\frac{\partial q}{\partial r} = 0, \quad r = 0 \tag{12}$$

$$q = 0, \quad t = 0 \tag{13}$$

$$q = q_e, \quad r = R_p, \quad t = \text{infinity} \tag{14}$$

The average resin-phase concentration is

$$\bar{q} = \frac{3}{R_p^3} \int_0^{R_p} q r^2 dr = \frac{(C_0 - C)V}{m} \tag{15}$$

Local equilibrium (q) existed between cAMP in the intraparticle stagnant solution and intraparticle surface. This equilibrium can be represented by the Langmuir adsorption isotherm, which is a mathematical relationship between C_e and q_e. The Langmuir adsorption isotherm is expressed by Eq. (7). Meanwhile, $\bar{q}$ was obtained in experiments by mass conservation. The partial differential equation of this model was numerically solved using PDESOL software.

The D_e was estimated by matching the experimental concentration decay data, C_{exp}, with the concentration decay predicted with a numerical solution of the diffusion model, C_{pred}. The best value for D_e was obtained when the diffusion model best fitted the experimental data, considering that the optimum fit was achieved by minimizing the following objective function

$$\text{Minimum} = \sum_{i=1}^{N} \left(\frac{C_{exp} - C_{pred}}{C_{exp}} \right)^2 \tag{16}$$

Also, the average absolute percentage deviation, %D, was calculated by applying the following equation

$$\%D = \frac{1}{N} \sum_{i=1}^{N} \left| \frac{C_{exp} - C_{pred}}{C_{exp}} \right| \times 100\% \tag{17}$$

3.4.2. Pseudo first-order and pseudo second-order kinetic models

In contrast to diffusion models, the kinetics of the adsorption of cAMP on D13 resin were studied using the prevailing equations, which were the Lagergren equations and regarded as pseudo first-order and second-order kinetic models [26,27]. The overall rate of adsorption in kinetic models is not considered to be controlled by any of the mass transport mechanisms, but by the surface adsorption rate. The overall rate of adsorption was represented in a similar fashion to the rate of a chemical reaction.

The pseudo first-order adsorption rate is expressed as

$$\frac{d\bar{q}}{dt} = k_1(q_e - \bar{q}) \tag{18}$$

This equation is integrated by the initial condition and the resulting equation is

$$q_e - \bar{q} = q_e e^{-k_1 t} \tag{19}$$

In logarithmic form

$$\ln(q_e - \bar{q}) = \ln q_e - k_1 t \tag{20}$$

The Lagergren equation can be rewritten as follows

$$\frac{C_0 - C_e}{m} - \frac{C_0 - C}{m} = \frac{C_0 - C_e}{m} e^{-k_1 t} \tag{21}$$

Further modification gives

$$C - C_e = (C_0 - C_e) e^{-k_1 t} \tag{22}$$

The adsorption rate for a second-order adsorption reaction can be represented by the following equation

$$\frac{d\bar{q}}{dt} = k_2(q_e - \bar{q})^2 \tag{23}$$

By integrating this equation, the following one is obtained

$$\frac{1}{q_e - \bar{q}} - \frac{1}{q_e} = k_2 t \tag{24}$$

Expressing the above equation in terms of C and C_e, the final equation is

$$C = C_0 - \left(\frac{m}{V} \right) \frac{k_2 \left[(V/m)(C_0 - C_e) \right]^2 t}{(1 + k_2[(V/m)(C_0 - C_e)]t)} \tag{25}$$

A comparison of the fit of the pseudo first-order, pseudo second-order, and Fick models to the experimental data for T = 283, 293, 303 and 313 K, C_0 = 5 g L^{-1} can be seen in Figs. 5–8 . From four dynamic plots at different temperatures, it was concluded that the concentration of the cAMP solution decreased gradually with time. By least square fitting, the effective diffusion coefficients at 283, 293, 303 and 313 K were 0.37×10^{-10}, 0.51×10^{-10}, 0.86×10^{-10} and 1.41×10^{-10} m^2 s^{-1}, respectively. The simulation was very successful and proved that the adsorption of cAMP onto D13 resin can be described by the Fick model. However, the fit of the pseudo first-order and pseudo second-order models to the experimental data were not as good as the Fick model according to the deviation in

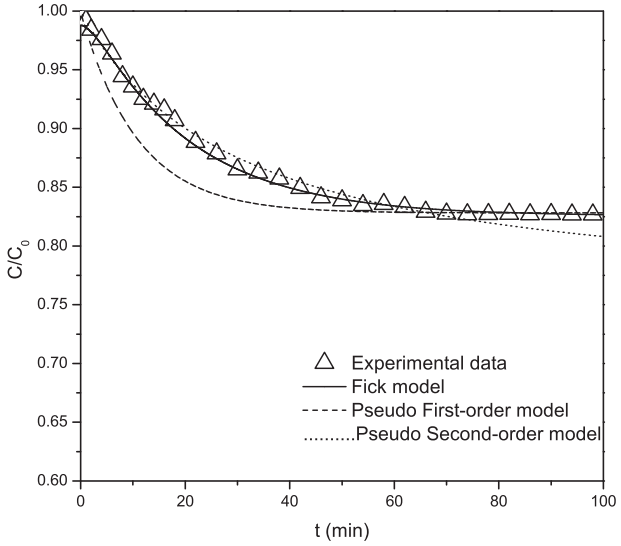

Fig. 5. Comparison of pseudo first-order, pseudo second-order, and Fick kinetic models for batch adsorption of cAMP by D13 resin at 283 K.

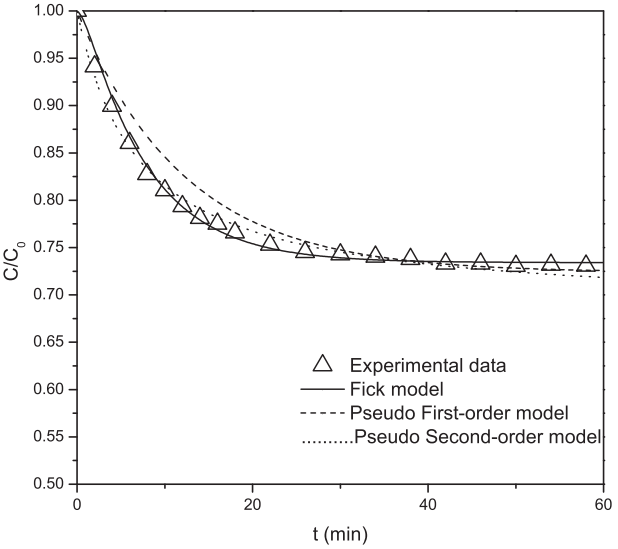

Fig. 7. Comparison of pseudo first-order, pseudo second-order, and Fick kinetic models for batch adsorption of cAMP by D13 resin at 303 K.

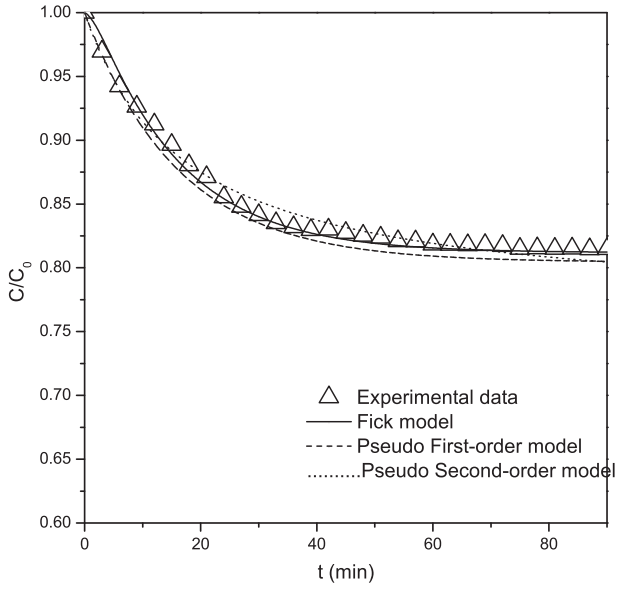

Fig. 6. Comparison of pseudo first-order, pseudo second-order, and Fick kinetic models for batch adsorption of cAMP by D13 resin at 293 K.

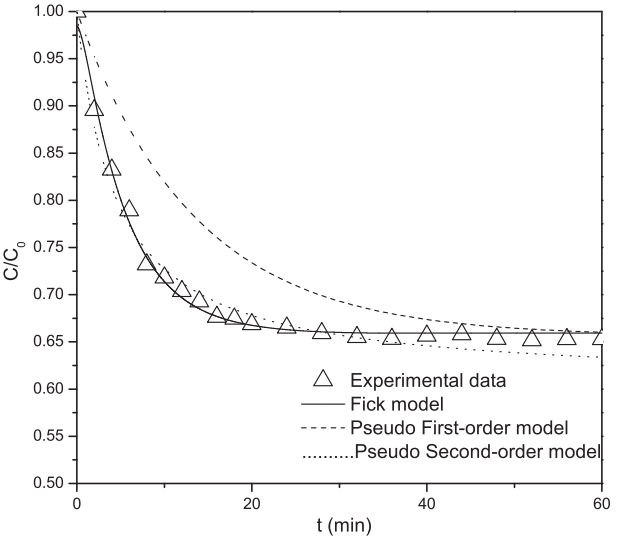

Fig. 8. Comparison of pseudo first-order, pseudo second-order, and Fick kinetic models for batch adsorption of cAMP by D13 resin at 313 K.

comparison (Table 3). It was concluded that the higher the temperature, the larger the effective diffusivity. The effective diffusivity (D_e) increased by 1.5–2-fold as the temperature increased by each 10 degrees in the range 283–313 K, although one study reported an increase of only 2-fold when the temperature increased by forty degrees [28]. However, in Table 3 the rate constants obtained from the pseudo first-order model varied with temperature without an obvious trend. Although the rate constants obtained from the pseudo second-order model revealed a increase trend, the average absolute percentage deviation %*D*, also had a large increase trend with the increase of temperature, which was ascribed to the comparatively large deviation for pseudo second-order model from experiment data in later stage of adsorption process.

In Table 4, it was concluded that the effective diffusivity (D_e) was stable when initial concentration varied at constant temperature. The effective diffusivity had no relationship with concentration, but

Table 3
Values of the rate constants for the pseudo first-order, pseudo second-order, and Fick kinetic models, $C_0 = 5\ g\ L^{-1}$.

T (K)	Pseudo first-order		Pseudo second-order		Fick model	
	k_1 ($\times 10^2\ min^{-1}$)	%*D*	k_2 ($\times 10^2\ min^{-1}$)	%*D*	D_e ($\times 10^{-10}\ m^2\ s^{-1}$)	%*D*
283	9.21	1.99	5.33	0.46	0.37	0.33
293	6.17	1.07	9.95	0.63	0.51	0.45
303	8.17	1.90	18.00	0.83	0.86	0.51
313	10.70	6.17	22.97	1.53	1.41	0.77

Table 4
Values of the rate constants for the pseudo first-order and pseudo second-order models and D_e for Fick kinetic model for different initial concentrations, T = 303 K.

C_0 (g L^{-1})	Pseudo first-order		Pseudo second-order		Fick model	
	k_1 ($\times 10^2$ min^{-1})	%D	k_2 ($\times 10^2$ min^{-1})	%D	D_e ($\times 10^{-10}$ m^2 s^{-1})	%D
1.8	5.51	1.72	10.11	1.03	0.85	0.72
2.4	6.23	1.46	12.02	1.12	0.81	0.58
4.2	6.94	2.13	14.24	0.88	0.84	0.47
5.0	8.17	1.90	18.00	0.82	0.86	0.51

the structure of adsorbent, temperature and adsorbate can affect effective diffusivity. In comparison, the rate constants k_1 and k_2 in pseudo first-order and pseudo second-order models proportionality increased with the concentration, but the relatively higher average absolute percentage deviation %D revealed that the simulation of these models is also worse than Fick model.

Fig. 9 describes the trend in concentration change versus different radius locations at various times including 20, 100, 400, 800 and 2000 s for 303 K and C_0 = 5 g L^{-1}. In early adsorption, due to the large concentration gradient inside the particle, the concentration from the outside layer to the inside layer changed dramatically. The cAMP molecule reached the core of the particle at 91 s, but it took 2000 s to reach adsorption equilibrium which was reflected on red color filling in the whole particle in Fig. 10 at 2000 s. (For interpretation of the references to color in this text, the reader is referred to the web version of the article.)

Fig. 10 shows the post-processing simulation data of intraparticle concentration distribution at various times including 20, 100, 400, 800 and 2000 s for T = 293 K and 303 K, C_0 = 5 g L^{-1}. These images vividly show that cAMP molecules gradually spread from the particle surface to the center of particle. In Fig. 10, concentration gradient became smaller and smaller as time went by until it was unchangeable. And at each time (20, 100, 400, 800 and 2000 s) concentration gradient of 293 K was always larger than that of 303 K before they all absolutely reached equilibrium. In addition, it was concluded that the higher the temperature, the larger the rate of dif-

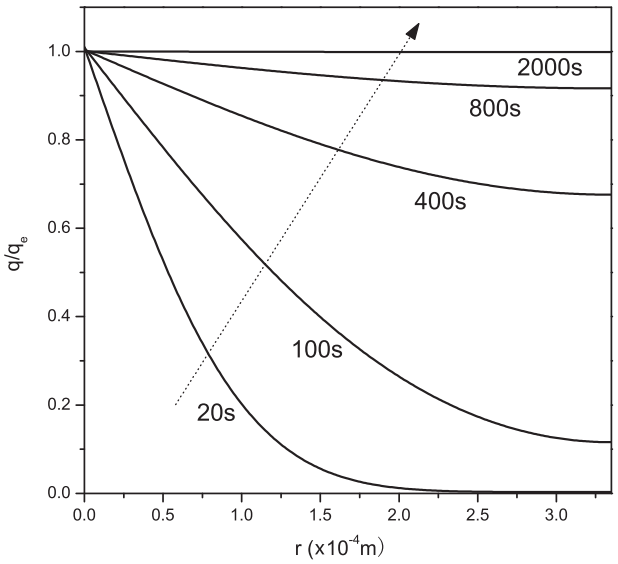

Fig. 9. Evolution of the dimensionless radial cAMP concentration profiles, C/C_0 versus r inside the particle calculated from the Fick model for batch adsorption at 303 K, C_0 = 5 g L^{-1}.

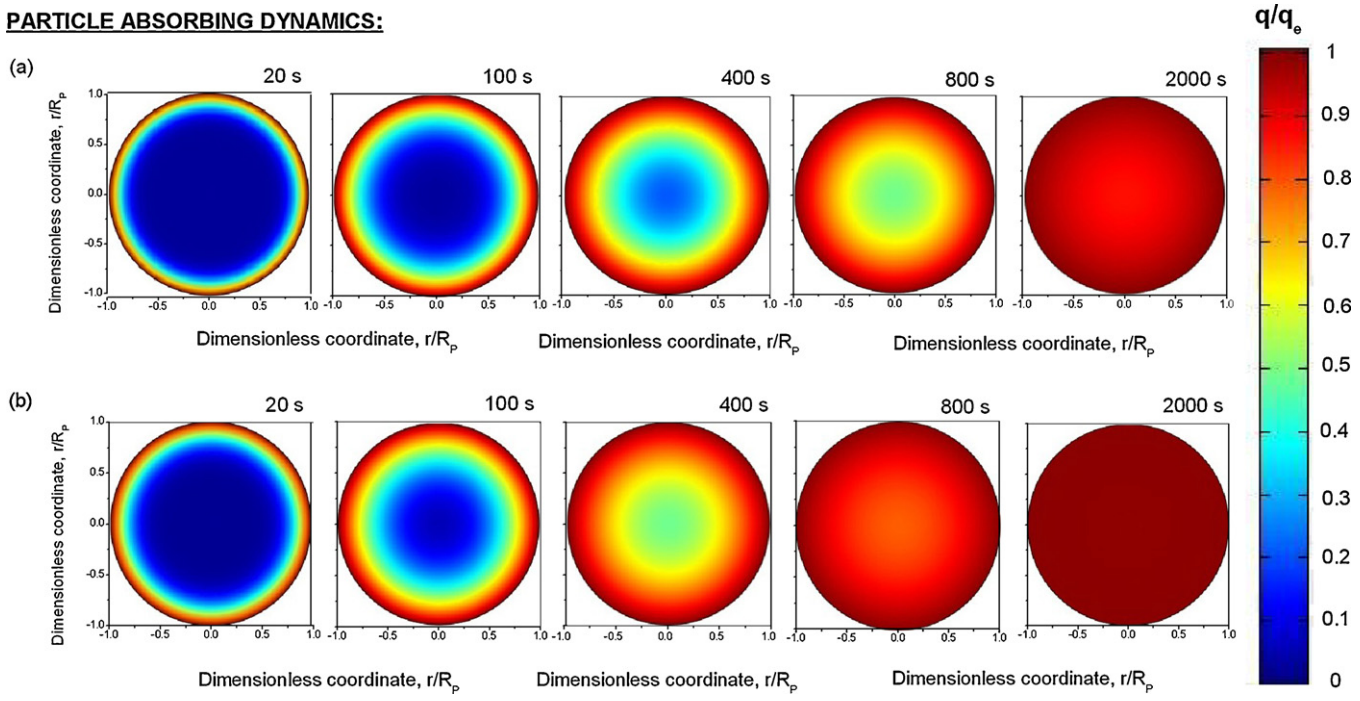

Fig. 10. Intraparticle two-dimensional profile of the concentration of the cAMP molecule in a 335 μm thick cross section through the center of a single particle during early adsorption at various times at (a) 293 K, C_0 = 5 g L^{-1} and (b) 303 K, C_0 = 5 g L^{-1}.

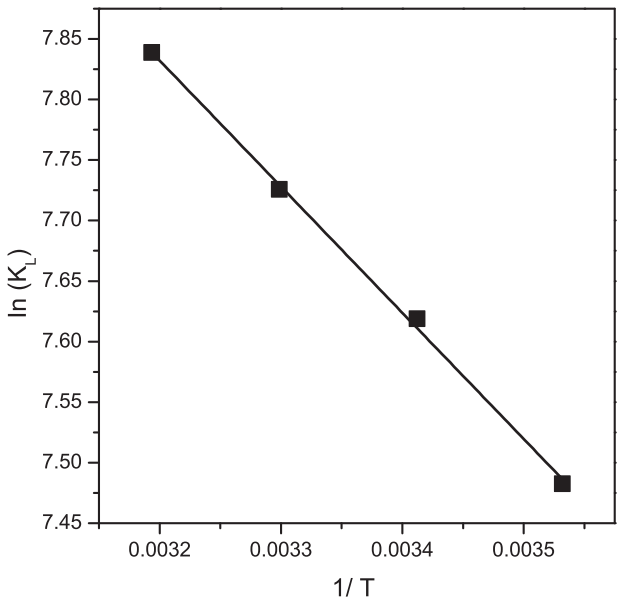

Fig. 11. Plot of $\ln K_L$ versus $1/T$ for predicting thermodynamic parameters during the adsorption of cAMP onto D13 resin.

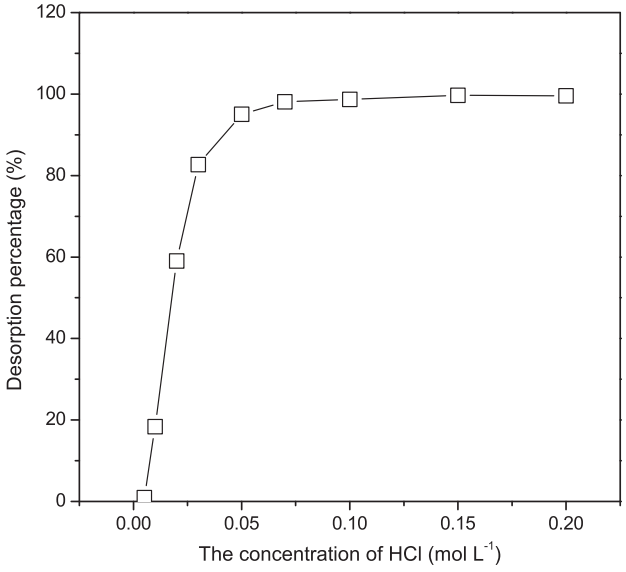

Fig. 12. The desorption percentage of cAMP from D13 resin using different concentrations of HCl solution, $T = 303$ K.

fusion, the larger the effective diffusion coefficient, although only eight images at 293 K and 303 K for different times are given here.

3.5. Thermodynamic parameters

In any adsorption procedure, both energy and entropy considerations should be taken into account in order to determine which process will take place spontaneously. The values of the thermodynamic parameters are the actual indicators for the practical application of a process. The amounts of cAMP adsorbed at equilibrium at different temperatures (283, 293, 303 and 313 K) were examined to obtain thermodynamic parameters for the adsorption system.

Because K_L is the Langmuir constant and its dependence on temperature can be used to predict thermodynamic parameters such as changes in Gibbs free energy (ΔG^0), enthalpy (ΔH^0) and entropy (ΔS^0) associated with the adsorption process, these parameters were determined by the following equations

$$\Delta G^0 = -RT \ln K_L \tag{26}$$

$$\ln K_L = -\frac{\Delta G^0}{RT} = -\frac{\Delta H^0}{RT} + \frac{\Delta S^0}{R} \tag{27}$$

The plot of $\ln K_L$ as a function of $1/T$ (Fig. 11) yielded a straight line from which ΔH^0 and ΔS^0 were calculated from the slope and intercept, respectively.

The overall free energy changes (ΔG^0) during the adsorption process were -17.61 kJ mol^{-1} at 283 K, -18.56 kJ mol^{-1} at 293 K, -19.46 kJ mol^{-1} at 303 K and -20.40 kJ mol^{-1} at 313 K, which were all negative, and corresponded to a spontaneous process of cAMP adsorption. The positive value for the enthalpy change ΔH^0 (+8.66 kJ mol^{-1}) indicated that the ion-exchange adsorption of cAMP onto D13 resin was physical in nature involving weak forces of attraction and was also endothermic [29]. Endothermic adsorption of cAMP has not been previously reported. The positive entropy change ΔS^0 (+92.84 J (mol K)$^{-1}$) corresponded to an increase in the degree of freedom of the adsorbed species.

3.6. Regeneration

The regeneration of resin D13 using 0.1 M HCl which can be ensured when desorption percentage of cAMP reached 99.0% is practicable in Fig. 12. Therefore, used resin should be soaked in 0.1 mol/L HCl solution for 8 h, making sure that all functional groups of resin take chloride ions again, then residual HCl on resin surface has to be rinsed by deionized water for several times as clearly as possible. The regenerated adsorbent was reused up to five adsorption–desorption cycles and the results are illustrated in Fig. 13. From this figure, it is clear that the amount of adsorbed cAMP remained almost constant throughout the five cycles. This may have been due to the negligible amount of D13 resin lost during the adsorption–desorption cycles. The decrease in efficiency of not more than 5% showed that the adsorbent was a good potential material to adsorb cAMP even after being reused several times. It indicated that the adsorption–desorption process using D13 resin was a reversible process.

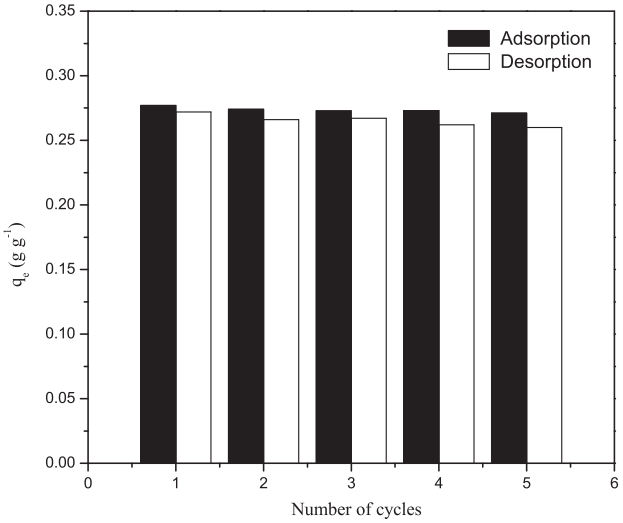

Fig. 13. The performance of D13 resin after multiple cycles, $T = 303$ K.

4. Conclusion

The pK_a of cAMP was estimated to be 3.7 for (–HPO^3), which provided reliable pK_a for cAMP in the analytical chemistry domain. pH 8 was the optimal pH for ion-exchange adsorption of cAMP onto D13 resin, and the maximum capacity reached was 0.1718, 0.1956, 0.2764 and 0.3437 g g^{-1} for 283, 293, 303 and 313 K, respectively. The adsorption data obtained were well described by the Langmuir adsorption isotherm model. The batch kinetics of cAMP adsorption onto an anion resin were simulated in this study in order to investigate its potential use as an effective adsorbent for cAMP separation and purification. Compared with the pseudo first-order and pseudo second-order, Fick kinetic model was more suitable for predicting the adsorption process. The effective diffusion coefficients (D_e) at 283, 293, 303 and 313 K were estimated to be 0.37×10^{-10}, 0.51×10^{-10}, 0.86×10^{-10} and 1.41×10^{-10} m^2 s^{-1}, respectively. These results indicated that higher temperatures considerably enhanced the adsorption capacity and adsorption process. This can be attributed to the 'intramolecular potential' of cAMP relevant to temperature which corresponds fierce molecular motion. In addition, negative ΔG^0 indicated that the adsorption of cAMP onto an anion-exchange resin was spontaneous and a positive value for ΔH^0 (+8.67 kJ mol^{-1}) showed that the adsorption was an endothermic reaction in nature.

Acknowledgements

This work was supported by the National Basic Reaearch Program of China (973 Program, 2007CB714305) and National High-Tech Research and Development Plan of China (863 Program, 2007AA100404).

References

[1] A. Moutinho, P.J. Hussey, A.J. Trewavas, R. Malhó, cAMP acts as a second messenger in pollen tube growth and reorientation, Proc. Natl. Acad. Sci. U.S.A. 98 (2001) 10481–10486.
[2] H. Ding, R.X. Peng, J.P. Yu, Role of the cAMP in immunological liver injury in mice: comparing LPS-induced model with LPS + BCG-induced model, Chin. Pharmacol. Bull. 19 (2003) 940–943.
[3] J. Ishiyama, Isolation of mutants with improved production of cAMP from *Microbacterium* sp. no. 205 (ATCC21376), Appl. Microbiol. Biotechnol. 34 (1990) 359–363.
[4] J. Ishiyama, Effects of metal ions on cyclic AMP production by *Microbacterium* sp. no. 205, Nihon Nogekagaku 55 (1981) 777–785.
[5] X.C. Chen, J.X. Bai, J.M. Cao, Z.J. Li, J. Xiong, L. Zhang, Y. Hong, H.J. Ying, Medium optimization for the production of cyclic adenosine 3′,5′-monophosphate by *Microbacterium* sp. no. 205 using response surface methodology, Bioresour. Technol. 100 (2009) 919–924.
[6] D. Butterworth, Clavulanic acid: properties, biosynthesis, and fermentation, in: E.J. Vandamme (Ed.), Biotechnology of Industrial Antibiotics, Marcel Dekker, New York, 1984, pp. 225–235.
[7] A. Shukla, Y.H. Zhang, P. Dubey, J.L. Margrave, S.S. Shukla, The role of sawdust in the removal of unwanted materials from water, J. Hazard. Mater. 95 (2002) 137–152.
[8] Z. Aksu, D. Akpinar, Simultaneous adsorption of phenol and chromium(VI) from binary mixtures onto powdered activated carbon, J. Environ. Sci. Health A35 (2000) 379–405.
[9] W. Qiu, Y. Zheng, Removal of lead, copper, nickel, cobalt, and zinc from water by a cancrinite-type zeolite synthesized from fly ash, Chem. Eng. J. 145 (2009) 483–488.
[10] Ö. Gök, A. Özcan, B. Erdem, A.S. Özcan, Prediction of the kinetics, equilibrium and thermodynamic parameters of adsorption of copper(II) ions onto 8-hydroxy quinoline immobilized bentonite, Colloids Surf. A: Physicochem. Eng. Aspects 317 (2008) 174–185.
[11] X. Li, L. Zhang, Y.H. Chang, S.B. Shen, H.J. Ying, P.K. Ouyang, Kinetics of adsorption of thymopentin on a gel-type strong cation-exchange resin, Chromatographia 66 (2007) 231–235.
[12] V. Chowdiah, G.L. Foutch, A kinetic model for cationic-exchange-resin regeneration, Ind. Eng. Chem. Res. 34 (1995) 4040–4048.
[13] M.J. Slater, The Principles of Ion Exchange Technology, Butterworth–Heinemann, Oxford, 1991.
[14] R. Leyva-Ramos, J. Rivera-Utrilla, N.A. Medellin-Castillo, M. Sanchez-Polo, Kinetic modeling of fluoride adsorption from aqueous solution onto bone char, Chem. Eng. J. 158 (2010) 458–467.
[15] G.A. Heeter, A.I. Liapis, Affinity adsorption of adsorbates into spherical monodisperse and bidisperse porous perfusive and purely diffusive adsorbent particles packed in a column parameter estimation in the Laplace transform domain, J. Chromatogr. A 760 (1997) 55–69.
[16] G.A. Heeter, Ph.D. Dissertation, The modelling and analysis of the dynamic performance of perfusion chromatography in fixed bed and periodic countercurrent column operations and parameter estimation and model discrimination using experimental data, Department of Chemical Engineering, University of Missouri-Rolla, Rolla, MO, USA, 1997.
[17] G. Stephanopoulos, K. Tsiveriotis, The effect of intraparticle convection on nutrient transport in porous biological pellets, Chem. Eng. Sci. 44 (1989) 2031–2039.
[18] R.M.C. Dawson, D.C. Elliott, W.H. Elliott, K.M. Jones, Data for Biochemical Research, Clarendon Press, Oxford, 1956.
[19] R.N. Goldberg, Y.B. Tewari, Thermodynamics of the hydrolysis reactions of adenosine 3′,5′-(cyclic)phosphate(aq) and phosphoenolpyruvate(aq); the standard molar formation properties of 3′,5′-(cyclic)phosphate(aq) and phosphoenolpyruvate(aq), J. Chem. Thermodyn. 35 (2003) 1809–1830.
[20] I. Marqués, G. Fonrodona, A. Baró, J. Guiteras, J.L. Beltrán, Study of solvent effects on the acid–base behaviour of adenine, adenosine 3′,5′-cyclic monophosphate and poly(adenylic) acid in acetonitrile–water mixtures using hard-modelling and soft-modelling approaches, Anal. Chim. Acta 471 (2002) 145–158.
[21] I. Langmuir, The adsorption of gases on plane surfaces of glass, mica and platinum, J. Am. Chem. Soc. 40 (9) (1918) 1361–1403.
[22] H.M.F. Freundlich, Überdie adsorption in lösungen, Z. Phys. Chem. 57 (1906) 385–470.
[23] M. Özacar, İ. Ayhan Şengil, H. Türkmenler, Equilibrium and kinetic data, and adsorption mechanism for adsorption of lead onto valonia tannin resin, Chem. Eng. J. 143 (2008) 32–42.
[24] K.R. Hall, L.C. Eagleton, A. Acrivos, T. Vermeulen, Pore- and solid-diffusion kinetics in fixed-bed adsorption under constant-pattern conditions, Ind. Eng. Chem. Fundam. 5 (2) (1966) 212–223.
[25] T.W. Weber, R.K. Chakravorti, Pore and solid diffusion models for fixedbed adsorbers, J. Am. Inst. Chem. Eng. 20 (2) (1974) 228–238.
[26] S. Lagergren, Zur theorie der sogenannten adsorption gelöster stoffe, Kungliga Svenska Vetenskapsakademiens Handlingar 24 (1898) 1–39.
[27] Y. Liu, Y.-J. Liu, Biosorption isotherms, kinetics and thermodynamics, Sep. Purif. Technol. 61 (2008) 229–242.
[28] P. Gluszcz, T. Jamroz, B. Sencio, S. Ledakowicz, Equilibrium and dynamic investigations of organic acids adsorption onto ion-exchange resins, Bioprocess Biosyst. Eng. 26 (2004) 185–190.
[29] Y. Yu, Y.-Y. Zhuang, Z.-H. Wang, Adsorption of water-soluble dye onto functionalized resin, J. Colloid Interface Sci. 242 (2) (2001) 288–293.